ISSN 1995-0780, Nanotechnologies in Russia, 2015, Vol. 10, Nos. 11–12, pp. 917–924. © Pleiades Publishing, Ltd., 2015.
Original Russian Text © A.A. Sivkov, I.A. Rakhmatullin, 2015, published in Rossiiskie Nanotekhnologii, 2015, Vol. 10, Nos. 11–12.

Plasmadynamic Synthesis of Dispersed Crystalline Phases in Supersonic Jet of Boron Carbon Electrodischarged Plasma

A. A. Sivkov and I. A. Rakhmatullin

Tomsk Polytechnic University, pr. Lenina 30, Tomsk, 634050 Russia

e-mail: riam@tpu.ru

Received June 30, 2015; in final form, August 13, 2015

Abstract—The possibility for the direct plasmadynamic synthesis of dispersed crystalline boron carbide in a supersonic jet of boron carbon electrodischarged plasma flowing into a chamber filled with argon at ambient pressure and temperature is shown. Phase composition is determined using X-ray diffraction. Particle morphology is shown using electron microscopy.

DOI: 10.1134/S1995078015060129

INTRODUCTION

Boron carbide is a super-hard material that attracts attention due to its refractoriness, chemical resistance to acids and alkalis, and low-density and low weight. In this regard, it is used as reinforcing additives in ceramics, for a cutting tool, as nozzles for abrasive blasting, and as a material that absorbs neutron radiation [1, 2].

The synthesis of boron carbide is implemented by a variety of different methods such as a carbothermic reduction [1, 2], mechanosynthesis [3], the sol-gel method [4], and gas-phase laser synthesis [5]. Most of these methods have a number of drawbacks: duration of the process; the need to implement high temperatures; and, consequently, energy consumption. One possible solution to these problems is the plasmodynamic method of synthesis (PDM). It is based on the use of a pulsed high-current coaxial magneto-plasma accelerator (CMPA) of erosion type [6]. The precursors required for synthesis may be introduced into high-current discharge plasma in different ways. For example, to obtain titanium nitride TiN, a reactor chamber (RC), to which a plasma shot is produced, is filled with nitrogen gas [7]. For obtaining titanium carbide TiC, the required amount of carbon in the form of powder is laid to the formation area of the plasma discharge structure at the beginning of the Carbon Cathode.

CMPA elaboration with graphite CE and CC is the development of PDM in the direction of obtaining carbon plasma jet and synthesis of carbon crystalline phases, as well as low-density ultrahard materials such as boron carbide B_4C [8].

This section presents the results of experimental studies of the possibility of plasmodynamic synthesis and obtaining crystalline boron carbide in the dispersed state according to the flowing of supersonic pulse jet of boron carbon electrodischarge plasma into a closed sealed volume filled with argon.

EXPERIMENTAL

Synthesis is implemented using high-current (~100 kA) pulse (~500 μs) CMPA of a hypervelocity jet of electrodischarge plasma flowing into an RC filled with argon under normal conditions. The power of the CMPA was carried out by the capacitive energy storage with a capacity of $C = 6.0$ mF at charging voltage of $U_{CHAR} = 3.0$ kV. In the experiment, oscillograms of the discharge current pulse and arc voltage were recorded and the curves of power and energy released in the experiment were constructed (Fig. 1).

The RC was opened and the powdered product was collected, the appearance of which is shown in Fig. 2, after about an hour after the shot. Upon loading 1.0 g of the powder mixture of precursors of amorphous boron and amorphous carbon (carbon black) in a weight ratio of 4 : 1, ~0.6 g of finely dispersed gray powder was collected from the RC.

RESULTS AND DISCUSSION

The X-ray diffraction (XRD) pattern in Fig. 3 is obtained using a Shimadzu XRD7000 X-ray diffractometer (0.15406 nm). An analysis of the resulting diffraction pattern of the product was carried out using a PowderCell2.4 program and PDF4+ structural database. The predominant crystalline phase is boron carbide B_4C (01-075-0424). Additionally, the presence of nanodispersed graphite-like carbon modification is seen in the product according to XRD-pattern

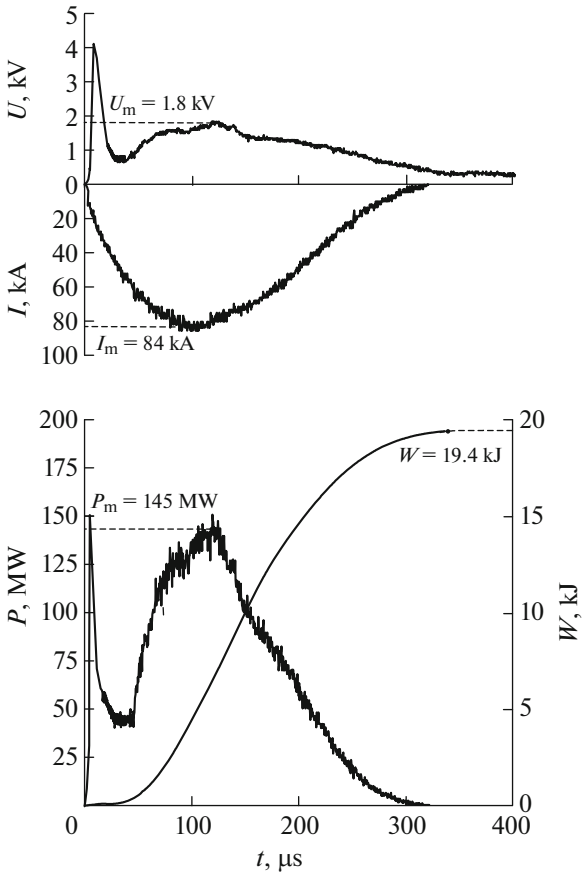

Fig. 1. Typical oscillogram.

Fig. 2. Photo of synthesized powder product.

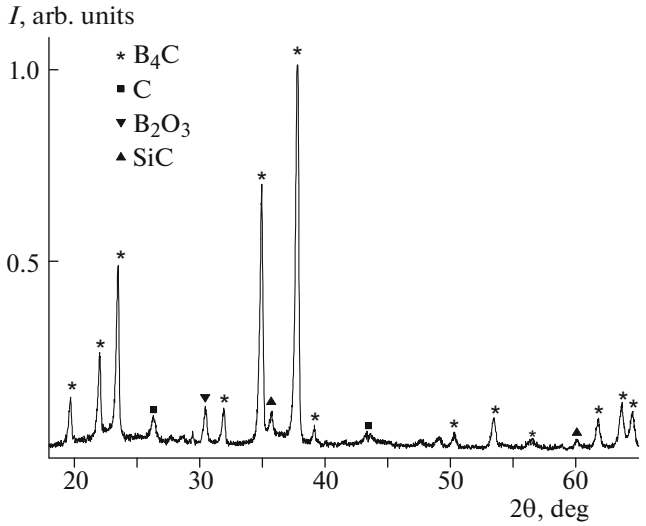

Fig. 3. X-ray diffraction pattern of the powder product of plasmodynamic synthesis in supersonic jet of boron carbon electrodischarge plasma flowing into free space.

(01-075-1621). Carbon excess is explained by the electrical erosion of the central electrode and the accelerating channel. Other low-intensity reflections marked on XRD-pattern show the presence of impurities in the form of nanostructured phases of silicon carbide SiC (00-029-1129) and boron oxide B_2O_3 (00-006-0297). Their presence at the level of traces is caused by the destruction of the reinforcing glass fiber of the insulator of the central electrode of the accelerator and small content of crystalline B_2O_3 in the original amorphous boron (precursor). Estimated quantitative calculation is carried out using the above structural models, whose results are presented in Table 1.

The presence of impurities generates the need to purify the synthesized product; however, in accordance with the works on the study of obtaining ceramics based on boron carbide, some procedures may be

Table 1. Evaluation results of full-profile X-ray analysis

Phase	Space group	wt %	Coherent scattering region(CSR), nm	$\Delta d/d^*10^{-3}$	Lattice parameters Theory/experiment	
					a	*c*
B_4C	R32m	96.0	45.0	0.58	5.6102/5.6103	12.1071/12.1070
g-C	P63mc	2.0	30.0	2.53	2.5294/2.5364	6.7651/6.7642
c-SiC	F43m	1.0	27.0	1.74	4.3480/4.3496	–
c-B_2O_3	P	1.0	30.0	0.59	10.055/10.1651	–

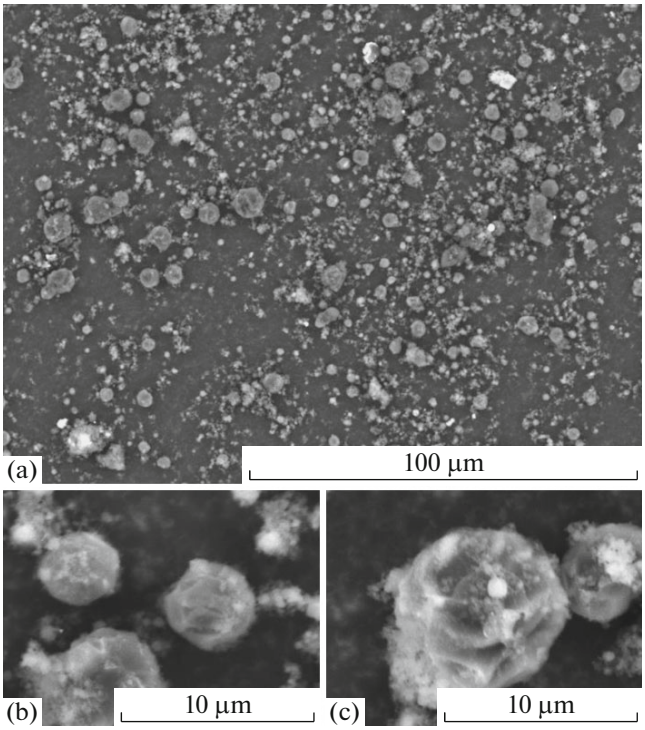

Fig. 4. SEM images of the powder product of plasmodynamic synthesis in the jet of boron carbon plasma flowing into the space with argon atmosphere.

eliminated, since the presence of a small amount of silicon carbide has a positive effect on the fracture toughness of ceramics produced by spark plasma sintering [9] and boron oxide can be removed by washing with boiling water [10]. Free carbon in the synthesized powder may also serve as an additive in sintering ceramics based on boron carbide, enabling the latter to correct mechanical properties [11].

Raster micrographs in Fig. 3, obtained on a Hitachi TM3000 scanning electron microscope, show that the powder has very broad polymodal size distribution with clearly distinguished two modes: coarse fraction from ~8.0 μm to ~200 nm and a fine fraction of less than ~100 nm. All particles have approximately the same contrast on the background of the carbon substrate, since the generally represented boron carbide phase is denser than graphite and other carbon structures. According to the images of relatively large particles greater than 1.0 μm, one can conclude that they have a single ordered facet of natural growth of crystals.

The phase belonging of the accessory-type crystal morphology determined by transmission electron microscopy (TEM) and microanalysis is based on the electron energy loss spectrum (EELS). Figures 5, 6, and 7 show the selected data in the form of bright-field and dark-field TEM images, as well as the pictures of

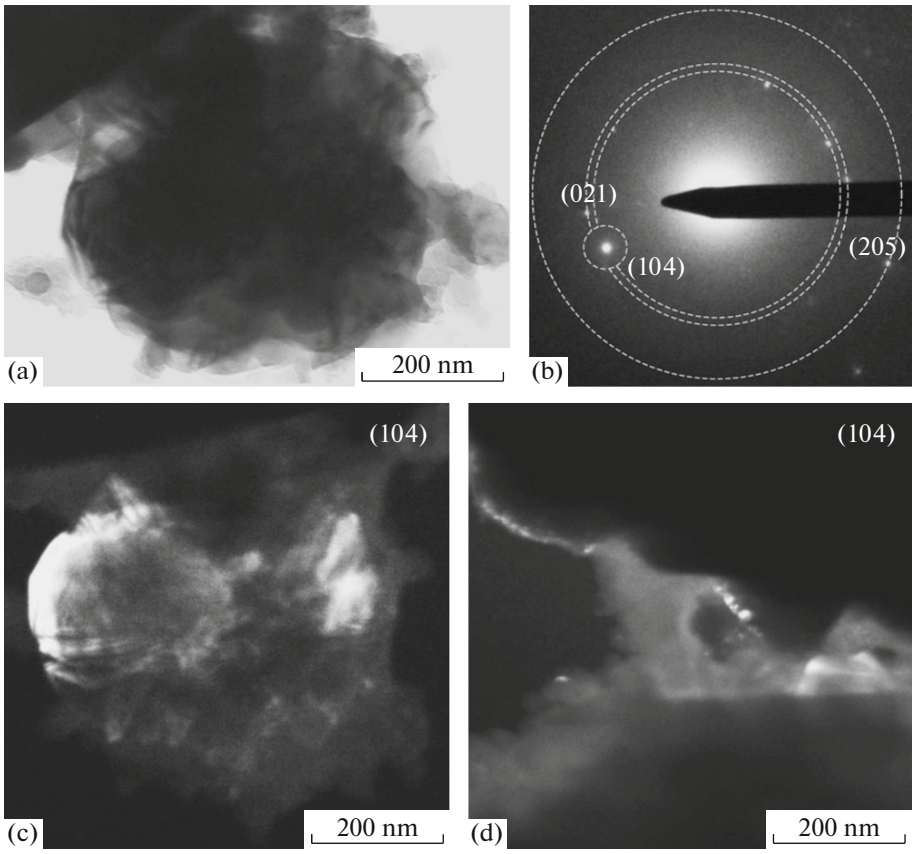

Fig. 5. TEM images of the product of PDM synthesis.

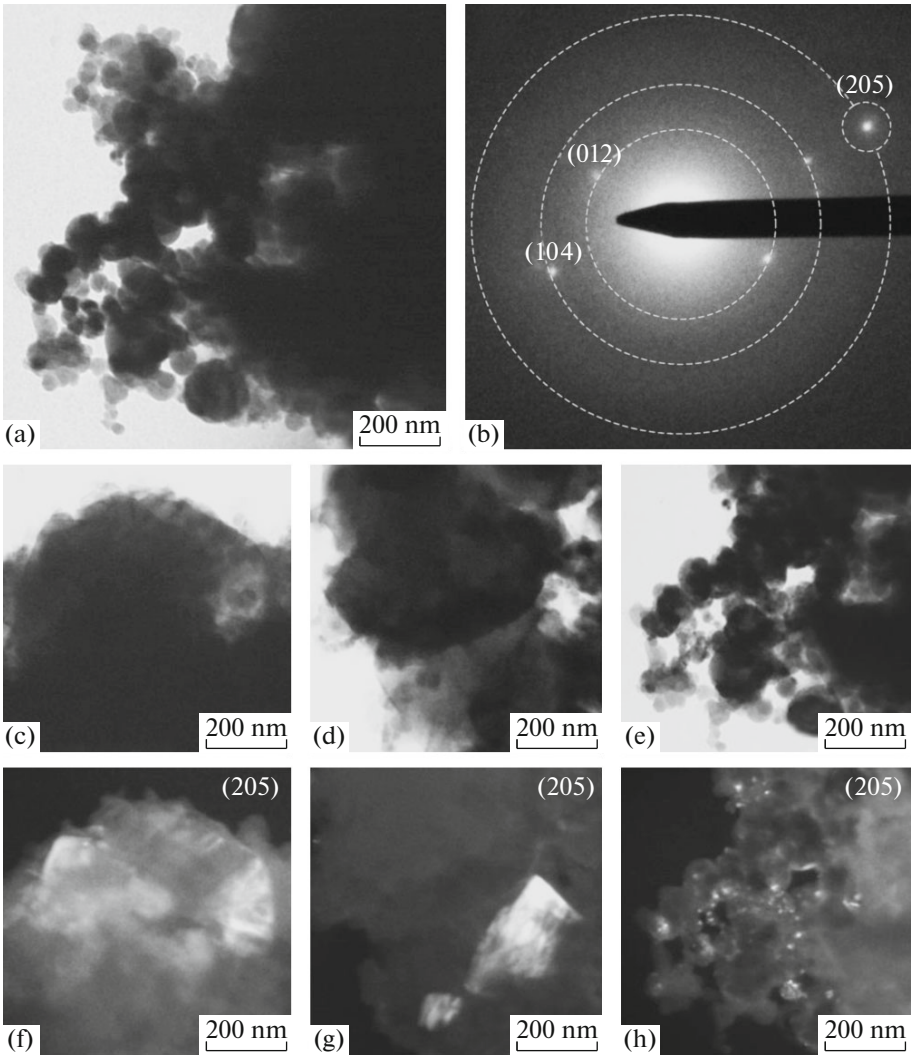

Fig. 6. TEM images of the product of PDM synthesis.

electron microdiffraction on the selected areas (SAED) obtained on a Philips CM12 microscope with accelerating voltage up to 100 kV. On bright-field TEM images (*a*) of such type, crystallites with sizes of about 1.0 μm are allocated only as dark figures because they are not transparent by electron beam. Rayed par-

Table 2. Comparison of the results of analysis of electron diffraction patterns

Experimental data d_{SAED}, nm	B_4C	
	d, nm	*hkl*
0.3787	0.3783	012
0.2573	0.2565	104
0.2410	0.2377	021
0.1714	0.1712	205
0.1404	0.14	220
0.1248	0.1257	217

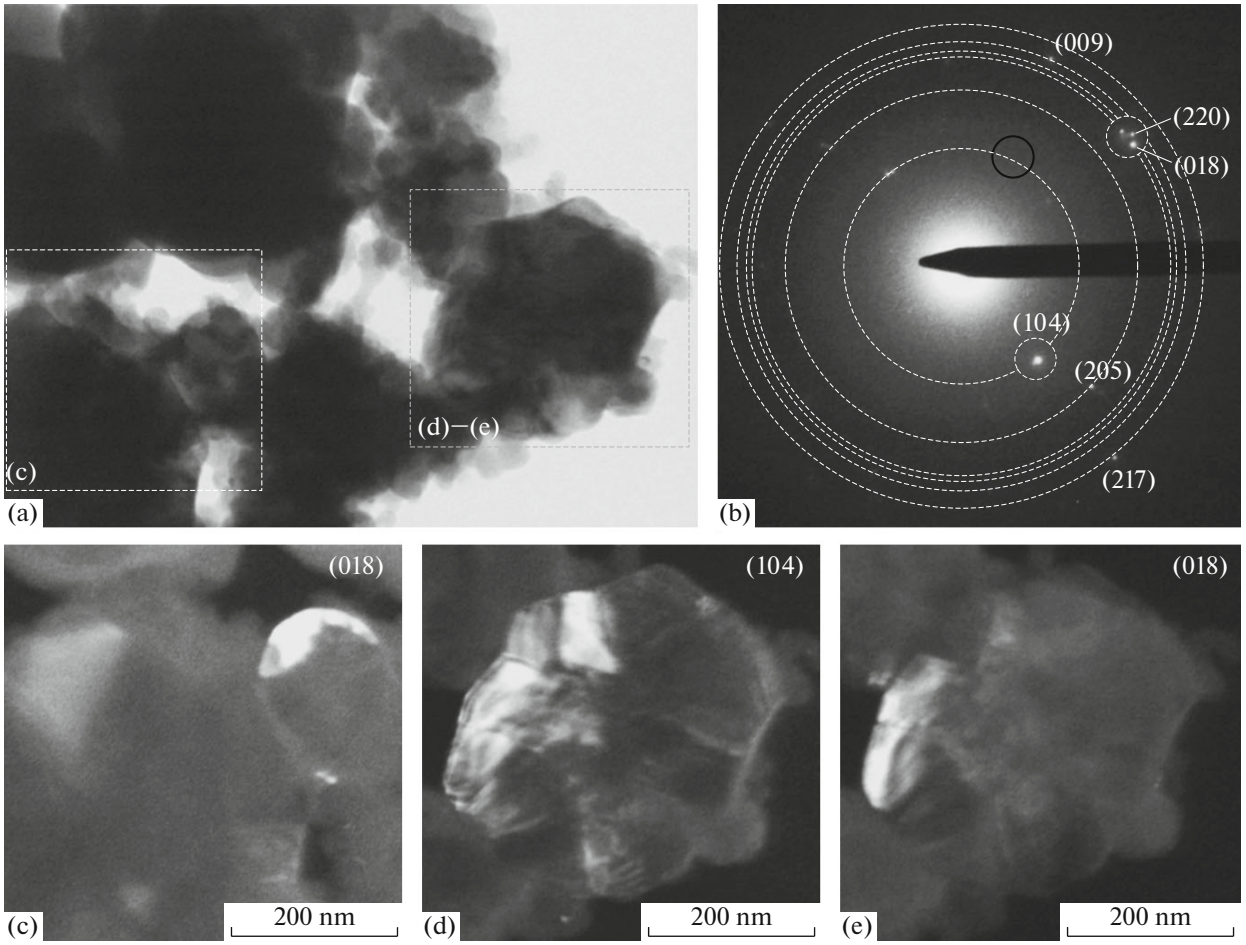

Fig. 7. TEM images of the product of PDM synthesis.

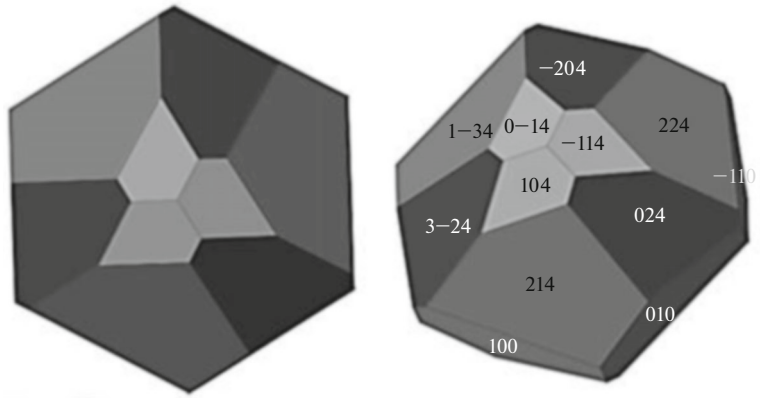

Fig. 8. Form of the crystals of trigonal–rhombohedral class.

ticles with sizes of about 100 nm segregate by complex crystal structure and morphology, comparable with the view of particles on scanning electron images in Fig. 4. Pictures of electron microdiffraction on the allocated areas with a predominance of this type of particles have a dot character. The most intense reflections on them are close enough to meet reflections on the systems of planes of the crystalline phase of boron carbide B_4C, as can be seen from Table 2. In this case, in dark-field TEM images obtained in diffracted

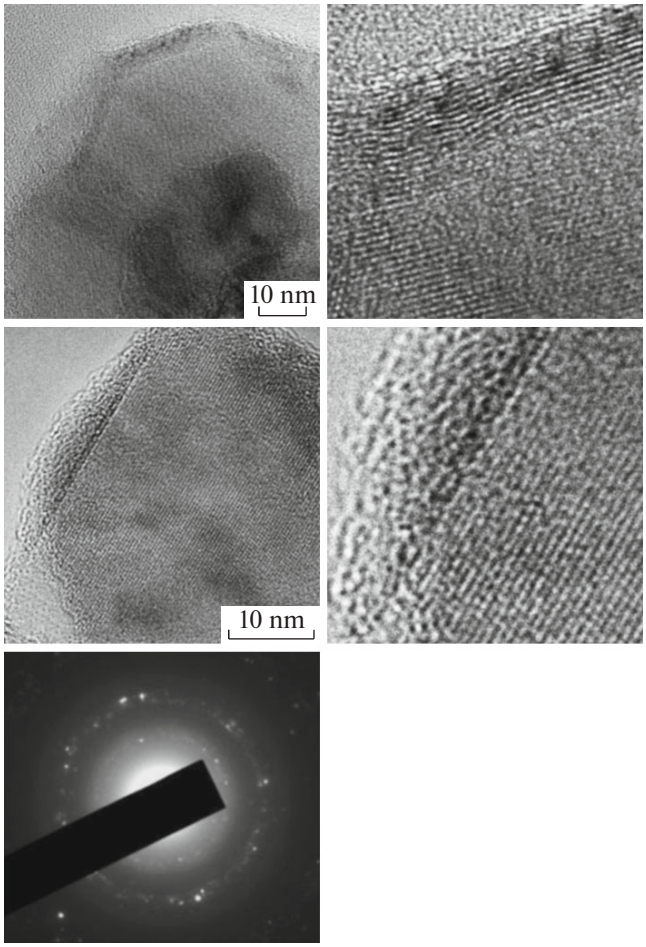

Fig. 9. HRTEM images of the product of PDM synthesis.

beams corresponding to marked reflexes, glow-reflecting planes in the bodies of particles are clearly visible. There is only the glow of narrow peripheral areas rayed by an electron beam for most particles (Fig. 5d). On dark-field images in Fig. 6e, very fine particles of boron carbide are dispalyed. Of particular interest are dark-field images in Figs. 5f, 6c, 7d, 7e, and 7f, where, in the light of the appropriate diffracted beams, contours of different crystallographic planes (104), (205), (018) glow in bodies of similar size and crystallite structure.

In our opinion, various SEM and TEM images of this type of crystallites are in good agreement with the theoretical concepts of morphology and structure of crystallites of trigonal–rhombohedral crystal system and R3m space group (Fig. 8), to which the crystalline phase of boron carbide B_4C refers.

Crystalline particles of this type have a shell with a thickness of less than ~10 nm from substantially amorphous or highly disordered crystalline material, as is shown in Fig. 9 with the data of transmission high resolution electron microscopy (HRTEM). In the particle bodies, interplanar distances of $d = 0.28$ nm and $d = 0.41$ nm, corresponding to the structural model of B_4C in two directions [110] and [003], are evaluated by direct measurement. In a weakly ordered multilayer shell, interlayer distances vary from 0.36 to 0.42 nm. Most likely, the shells of the particles are composed of carbon. Therefore, quantitative elemental analysis carried out by the EELS spectrum of electron energy loss (Fig. 10) overestimates the content of carbon with respect to the stoichiometry of boron carbide. Moreover, the presented picture of electronic microdiffraction confirms that particles belong to the crystalline phase of B_4C.

Except for the type of particles considered above, the product of plasmodynamic synthesis contains spherical particles reaching ~50 nm in size purely amorphous and with crystalline inclusions, as is shown in Fig. 11. Microdiffraction on such particles contains only multiple reflections close to respective nanoscale carbon structures and does not contain reflections belonging to B_4C. Amorphous particles have a highly disordered crystal shell with an average value of the interlayer distances of about 0.36 nm.

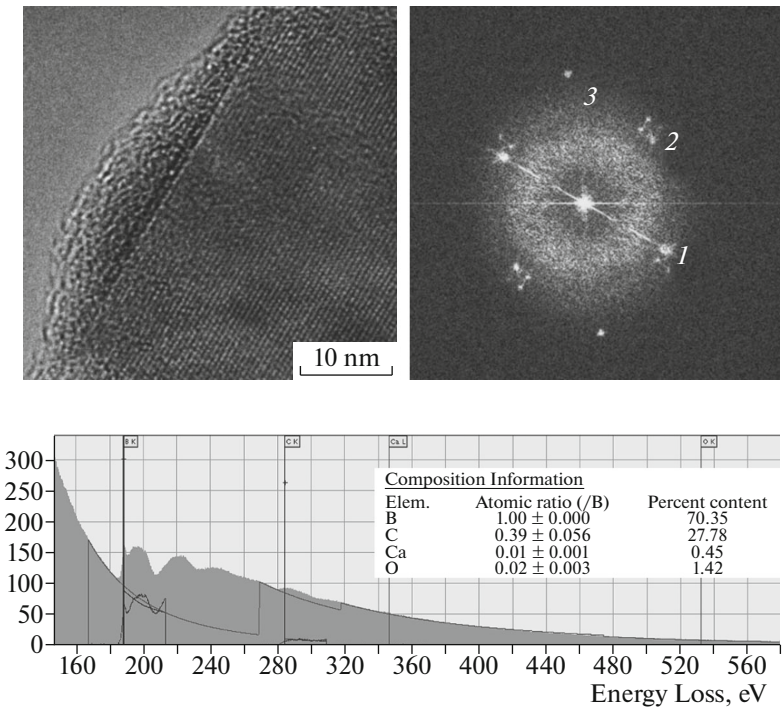

Fig. 10. HRTEM images of the product of PDM synthesis and its EELS range.

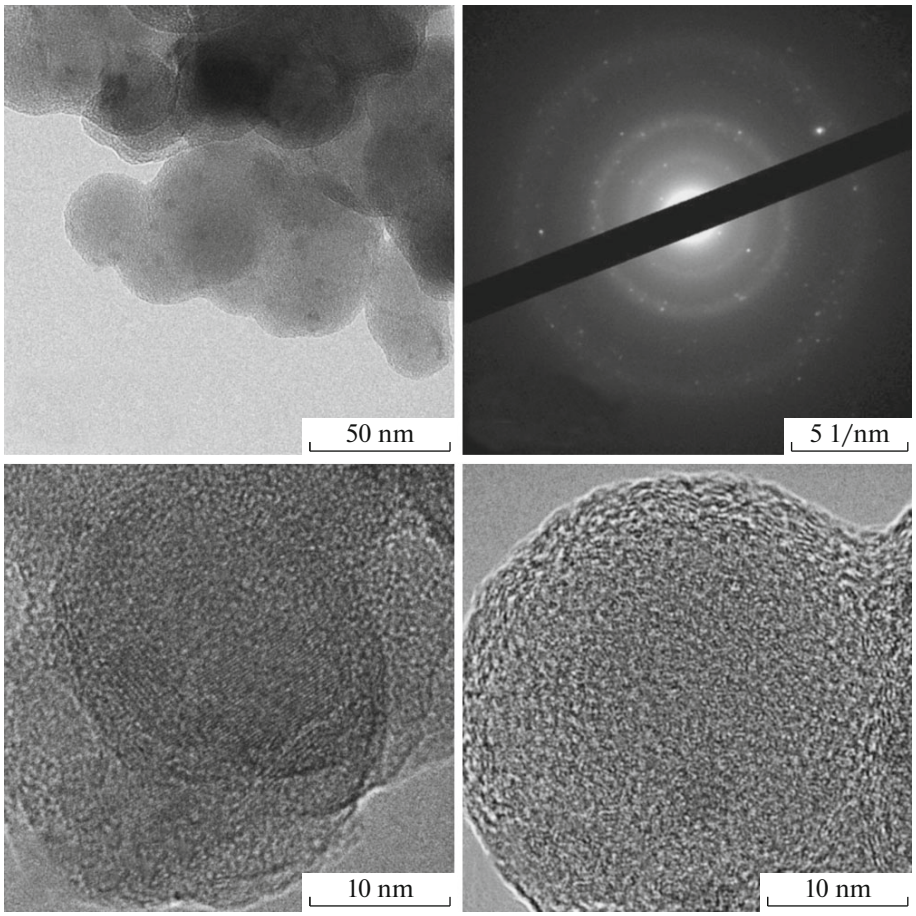

Fig. 11. HRTEM images of the product of PDM synthesis.

CONCLUSIONS

Thus, the data SEM, TEM, and HRTEM are consistent with the results of X-ray analysis and confirm the possibility of using PDM synthesis based on CMPA to obtain ultrafine crystalline boron carbide with a low content of impurities. In our opinion, various SEM and TEM images of the crystallites B_4C are in good agreement with the theoretical concepts of morphology and structure of crystals of the trigonal–rhombohedral system and R3m space group (Fig. 8).

ACKNOWLEDGMENTS

This work was supported by the Russian Science Foundation (project no. 15-19-00049).

REFERENCES

1. S. Chen, D. Z. Wang, J. Y. Huang, and Z. F. Ren, "Synthesis and characterization of boron carbide nanoparticles," Appl. Phys. A **79**, 1757–1759 (2004).
2. M. Kakiage, N. Tahara, I. Yanase, and H. Kobayashi, "Low-temperature synthesis of boron carbide from condensed boric acid-glycerin product," Mater. Lett. **65**, 1839–1841 (2011).
3. E. M. Sharifi, F. Karimzadeh, and M. H. Enayati, "Mechanochemical assisted synthesis of B4C nanoparticles," Adv. Powder Technol. **22**, 354–358 (2011).
4. A. Najafi, F. Golestani-Fard, H. R. Rezaie, and N. Ehsani, "A novel route to obtain B4C nano powder via sol-gel method," Ceram. Int. **38**, 3583–3589 (2012).
5. T. Oyama and K. Takeuchi, "Gas-phase synthesis of crystalline B4C encapsulated in graphitic particles by pulsed-laser irradiation," Carbon **37**, 433–436 (1999).
6. A. A. Sivkov, A. S. Saigash, A. A. Evdokimov, and A. Ya. Pak, "Direct synthesis of nanodispersed powders and compositions in hyperspeed flow of electric discharge plasma," Nanotekh., No. 2 (18), 38–43 (2009).
7. A. A. Sivkov, D. Yu. Gerasimov, A. S. Saigash, and A. A. Evdokimov, "Synthesis of superhard nanodispersed titanium compounds in a magnetoplasma accelerator operating in pulse-periodic regime," Russ. Phys. J. **54**, 1160 (2011).
8. A. A. Sivkov and A. Ya. Pak, RF Patent No. 2431947 RF H05H 11/00 F41B.
9. Yu. G. Tkachenko, V. F. Britun, E. V. Prilutskii, D. Z. Yurchenko, and G. A. Bovkun, "Structure and properties of B4C-SiC composites," Powder Metall. Met. Ceram. **44**, 196–201 (2005).
10. S. W. Du, A. I. Y. Tok, and F. Y. C. Boey, "RF Plasma synthesis of boron carbide nanoparticles," Solid State Phenom. **136**, 23–28 (2008).
11. R. Riedel and I. W. Chen, *Ceramics Science and Technology*, Vol. 2: *Materials and Properties* (Wiley, New York, 2011), p. 888.

Translated by Sh. Galyaltdinov